Title

Measuring the effects of pore-pressure changes on seismic amplitude using crosswell continuous active-source seismic monitoring (CASSM)

Authors
Marchesini, Pierpaolo
Daley, Thomas
Ajo-Franklin, Jonathan

Publication Date
2017-08-17

DOI
10.1190/segam2017-17792031.1

Measuring the effects of pore pressure changes on seismic amplitude using cross-well Continuous Active-Source Seismic Monitoring (CASSM)

Pierpaolo Marchesini, Thomas M. Daley, and Jonathan B. Ajo-Franklin*
Lawrence Berkeley National Laboratory (LBNL), Energy Geosciences Division

Summary

Monitoring of time-varying reservoir properties, such as the state of stress, is a primary goal of geophysical investigations, including for geological sequestration of CO_2, enhanced hydrocarbon recovery (EOR), and other subsurface engineering activities. In this work, we used Continuous Active-Source Seismic Monitoring (CASSM), with cross-well geometry, to measure variation in seismic coda amplitude, as a consequence of effective stress change (in the form of changes in pore fluid pressure). To our knowledge, the presented results are the first *in-situ* example of such crosswell measurement at reservoir scale and in field conditions. Data compliment the findings of our previous work which investigated the relationship between pore fluid pressure and seismic velocity (velocity-stress sensitivity) using the CASSM system at the same field site (Marchesini et al., 2017, *in review*). We find that P-wave coda amplitude decreases with decreasing pore pressure (increasing effective stress).

Introduction

In recent literature, many examples of time-lapse or 4D seismic surveys focused on monitoring changes in reservoir properties by way of induced variation in seismic wave propagation (Landro and Stammeijer, 2004; Vasco, 2004; Sayers, 2006; Duffaut, et al., 2011; Trani, et al., 2011). Several attributes of the seismic wavefield were measured and studied, including attenuation, amplitude, phase, and velocity. In particular, the reduction of coda (post P-wave) amplitude has been associated with the decrease of fluid pore pressure (Valstos et al., 2006), with compliant pores or small cracks closing under the effect of higher effective stress. The majority of published work on amplitude as a function of varying stress at reservoir conditions has been conducted in lab settings on core samples. While lab measurements remain crucial to our understanding, often the process of obtaining cores can lead to alterations during recovery and storage, in the form of secondary micro-cracking due to gas exsolution (like in the case of deep shale formations, Holt et al., 2005). Sams et al. (1997) show how the velocity dispersion in systems with micro-cracks provides a further source of uncertainty, preventing lab measurements from optimally calibrating field measurements. This effect is related to the use of ultrasonic frequencies (10^5 to 10^6 Hz) for lab measurements, which are not compatible with the usual practice in seismic surveys (1 to 10^3 Hz).

Field scale measurement at high effective pressure are needed to overcome all these problems. However, *in-situ* seismic monitoring mostly relies on surface measurements of reflection amplitudes to remotely estimate varying reservoir properties (Arts et al., 2004; Majer et al., 2006; Williams and Chadwick, 2012; White, 2013; Arogunmati and Harris, 2014). Several factors limit the ability of remote measurements using surface seismic to produce reliable results, including the lack of resolution (Johnston, 2013), the presence of multiples and attenuation (Campbell et al., 2005), and, more in general, reservoir compaction (Guilbot and Smith, 2002).

Cross-well CASSM has been applied in several field studies to detect stress-induced seismic velocity changes for earthquake monitoring (Silver et al., 2007; Niu et al., 2008), to track changes in reservoir fluid saturation (Daley et al., 2010), and to monitor shallow hydraulic fracture nucleation (Ajo-Franklin et al., 2011). In this work, cross-well CASSM is used to measure and monitor pressure-induced seismic amplitude variation after fluid withdrawal within a ~3.2 km deep reservoir unit (Figure 1).

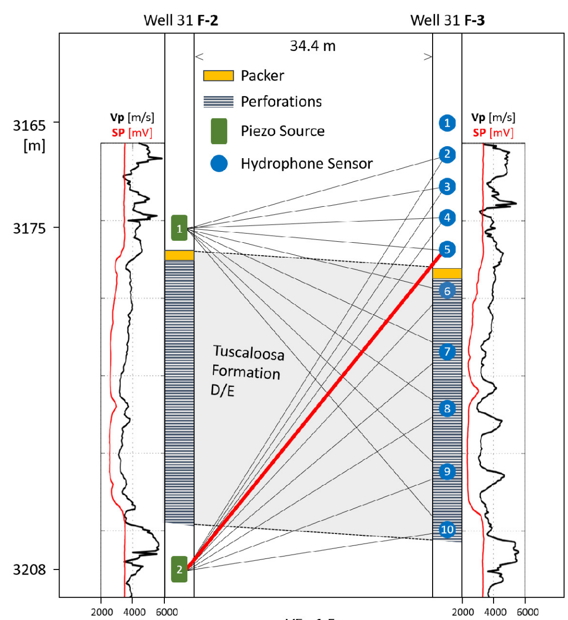

Figure 1: Schematic representation of CASSM data acquisition at the Cranfield field site. Raypaths from sources to hydrophone sensors are shown in black. Hydrophone sensor #1 failed during

installation. Data shown in Figures 2, 3 and 4 are from the raypath shown in red (source #2 to sensor #5). Modified from Marchesini, et al. (2017, *in review*).

Results from three discrete fluid pumping events show a direct correlation between seismic amplitude and downhole fluid pore pressure, indicating a decrease of post P-wave amplitude correspondent to a decrease in pore fluid pressure.

Field Site Description and Data Acquisition

The CASSM system was deployed at Cranfield field site, located near Natchez, Mississippi. The site was part of a Detailed Area Study (DAS) in a CO_2 sequestration test performed by the Southeast Regional Carbon Sequestration Partnership (SECARB). The DAS site includes three boreholes, an injection well (not part of this study) and two monitoring wells (31 F-2 and 31 F-3, Figure 1).

Changes of pore fluid pressure were induced by three discrete fluid withdrawal events during the CASSM monitoring time interval of ~5 days in a 24 m-thick, perforated, and packer-isolated interval within the lower Tuscaloosa Formation (layer D/E). The formation is mainly composed of fluvial sandstone with high vertical and lateral heterogeneity (25% porosity, 50 mD - 1000 mD permeability) located in an anticlinal four-way closure at a depth of ~3.2 km. The bottom hole well spacing (31 F-2 to 31 F-3) was measured as 34.4 m. Two piezo-electric seismic sources (described in Daley et al., 2007) were deployed in well 31 F-2, concentric on the 2.875" production tubing, and two, 5-elements hydrophone arrays were deployed in well 31 F-3 on production tubing.

A set of 25 stacks were acquired for each piezo-electric source every 5 minutes, giving the experiment a very high temporal resolution. A schematic representation of the acquisition geometry in shown in Figure 1. Following an initial pressure test of well head and blow out preventer, reservoir fluids were produced from well 31 F-2 (using the production tubing, through the CASSM sources). Fluids were produced in three discrete events using a nitrogen lift procedure (Figures 2, 4, pumping events #1, #2, #3). A total of 876 barrels of fluid were produced from the well over three days. Downhole pressure was monitored and recorded with a quartz pressure/temperature gauge installed on production tubing and placed within the perforated zone of the reservoir. This pressure data is used as a measure of pore fluid pressure.

Discussion of Results / Conclusions

Figure 2 shows results from the work by Marchesini et al. (2017, *in review*), which investigated the *in-situ* relationship between pore fluid pressure and P-wave velocity in the same field site and with the same cross-well data. The correlation between variation in first arrival time delays (i.e. variation in velocity) and pore pressure changes is interpreted as the velocity-stress sensitivity measured in the reservoir. Time delays were computed by cross-correlating each trace with the first trace in the sequence to obtain the delay time of the first arrival for each source-sensor pair at 5 minute intervals (cross-correlation evaluation window = 13.2 ms - 14.9 ms, Figure 3, Window P). The comparison between variation of time delays and pore pressure changes, revealed also a drift in baseline travel time delay correlated with individual pumping events, suggestive of a secondary process happening in the formation (Figure 2, green).

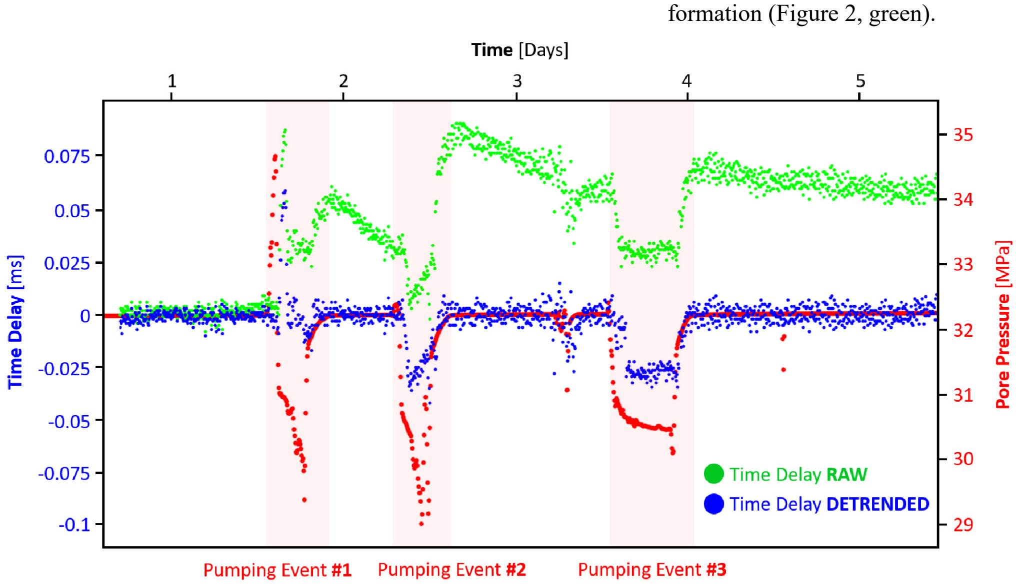

Figure 2: Temporal variation in cross-well time delay for the raypath from source #2 to sensor #5 (green = raw data; blue = detrended data), with bottom-hole fluid pressure (red), over ~5 days of monitoring. Data were detrended by applying an adaptive median filter to correct for a secondary process (likely gas exsolution) at the end of each discrete pumping event. Modified from Marchesini, et al. (2017, *in review*)

Effects of pore pressure changes on seismic amplitude

This mechanism has been hypothesized as gas exsolution since the pore water is known to be saturated with methane (CH_4). The gas exsolution process produces a further increase in delay time. In between pumping events the time delays decrease following a dissolution trend. Raw data were detrended by applying an adaptive median filter that corrects for individual exsolution effects and dissolution trends (Figure 2, blue).

Results from time delay analysis encouraged further work on the dataset. The variation of seismic RMS amplitude was compared to the pore fluid pressure changes. Vlastos et al. (2006) performed theoretical simulations of fluid flow in a fractured media, computing the elastic response corresponding to stepwise pore pressure changes. This work indicates a different response between P- and S-waves and coda (or scattered) waves to pore pressure changes. Results show that P-waves seem to be less affected (or affected in a limited way), while S- and coda waves are strongly affected.

Following these findings, we chose a different evaluation window for the RMS amplitude computation for each trace of the dataset = 18.8 ms - 20.5 ms (Figure 3, Window C). This window had the maximum pressure effect on seismic amplitudes. The evaluation window is in the P-wave coda, before the direct S-wave and may be P-to-P, P-to-S or S-to-P scattering. Figure 4A shows results from the comparison between the pore fluid pressure changes and seismic RMS amplitude in window C, while Figure 4B illustrates the RMS computed with the P-wave window used for the time delays (Figure 3, Window P). Anomalous amplitude values are the reason for the removed data points at day ~3.2.

Like in the case of time delays, data show a strong correlation between RMS amplitudes variation and pore pressure changes, corroborating the results of Marchesini et al. (2017, *in review*), and indicating that seismic amplitude could be used as proxy for stress state in the subsurface at field scale and reservoir conditions (Figure 4A).

Data show that a decrease of pore fluid pressure is matched by a decrease of coda event amplitude during periods of pumping events, suggesting that scattering amplitude is inversely dependent to rock stiffness. In fact, lower pore pressure means higher effective stress (given a constant confining pressure): the closing of compliant pores (or small cracks) which will increase the rock stiffness, therefore decreasing the scattering seismic response.

When comparing Figure 2, detrended data (blue) versus Figure 4, Panel A, data show that:

1) In periods of constant pore fluid pressure, the fluctuation of RMS amplitudes around their mean value is more pronounced than in time delay data. In other words, RMS amplitude measurements are more scattered and less stable than time delay equivalent;
2) Despite showing a short spike in correspondence with pumping event #1, RMS amplitudes are less reactive to rapid and spurious pore pressure changes, as compared to time delays.
3) RMS amplitude data show a drift from their baseline, indicative of the gas exsolution process. The effect is more pronounced in pumping events #1 and #2, while it decreases in magnitude for pumping event #3, where the system starts returning to its original baseline amplitude state;

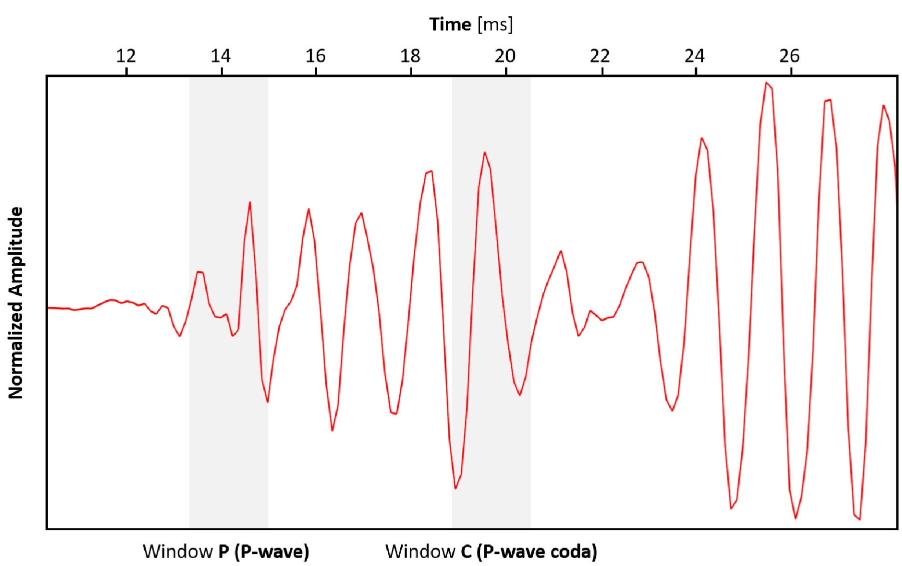

Figure 3: Sample trace recorded for the raypath from source #2 to sensor #5, and corresponding to day 2.5 (see Figures 2, 4). The amplitude of the waveform is normalized to the max amplitude in the dataset. Window P indicates the evaluation window (from 13.2 ms to 14.9 ms) for the first arrival, and used for computing the cross-correlation in the time delay analysis. Window C indicates the evaluation window (from 18.8 ms to 20.5 ms) centered in the P-wave coda, and used for computing the RMS amplitude for all the traces in the dataset.

4) The RMS amplitude dataset shows a generalized delay in response to pore pressure changes. In other words, the seismic amplitude dataset is shifted with respect to the pressure data. The same behavior was observed in the time delay dataset. Marchesini et al. (2017, *in review*) quantified this delay as ~45 minutes.

Figure 4B shows the RMS amplitude variation computed using Window P (13.2 ms - 14.9 ms, Figure 3), centered around the P-wave first arrival, and used also to compute the cross-correlation in the time delays analysis (Figure 2). When compared to the equivalent RMS amplitude variation computed on Window C, data show that the pore pressure change effect on amplitude variation is null, or at least orders of magnitude less than in Figure 4A, corroborating the modeling results of Valstos et al. (2006).

This finding, based on our field observations, has important consequences on exploration techniques involving amplitude analysis. For such cases, the approach should consider coda wave data in order to detect even small changes in pore pressure, which are important for CO_2 storage and EOR.

Acknowledgements

We thank the Southeast Regional Carbon Sequestration Partnership (SECARB) and all their partners for their support. This research was supported by the Assistant Secretary for Fossil Energy, Office of Natural Gas and Petroleum Technology, SECARB program and CSRP/GEO-SEQ Program, through the National Energy Technology Laboratory of the U.S. Department of Energy, under the U.S. DOE Contract No. DE-AC02-05CH1123.

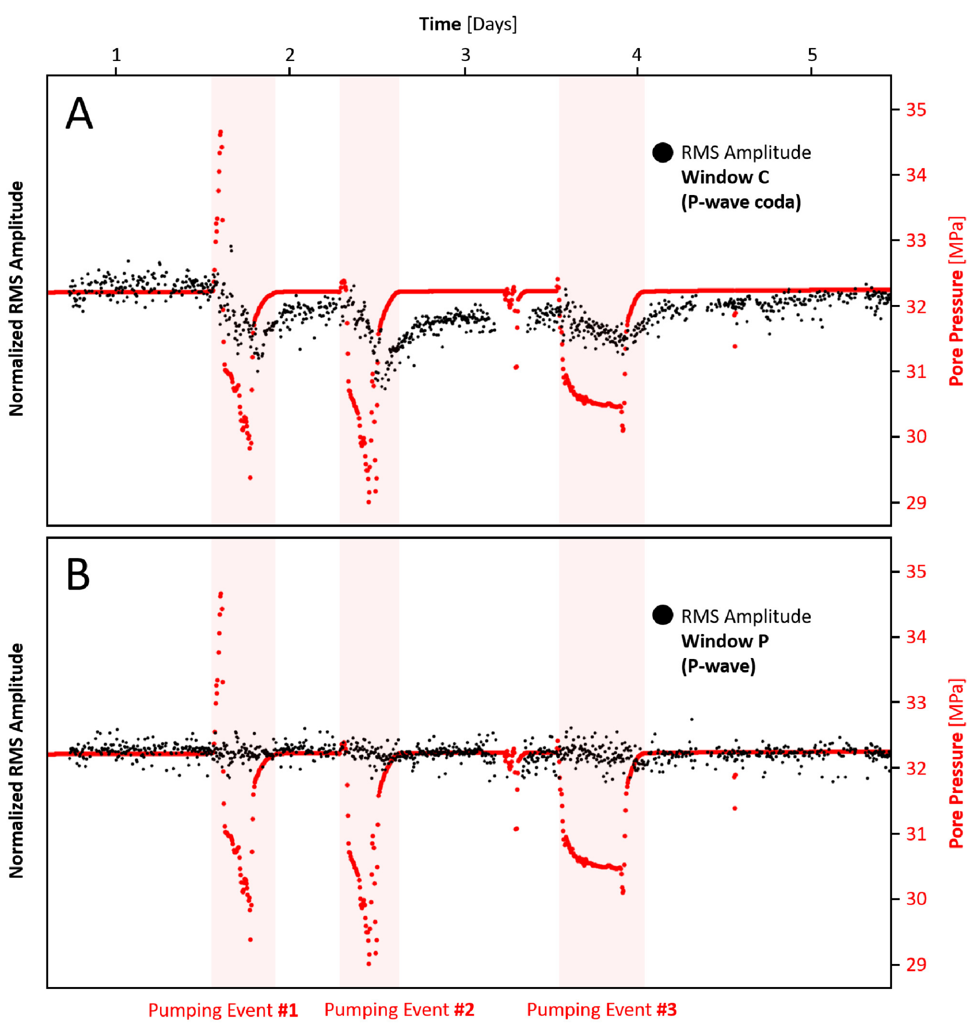

Figure 4: Temoral variation in cross-well RMS amplitude for the raypath from source #2 to sensor #5, with bottom-hole fluid pressure (red), over ~5 days of monitoring. The amplitude of the waveform is normalized to the max amplitude in the dataset.

Panel A shows the RMS amplitude computed using an evaluation window equal to Window C, from 18.8 ms to 20.5 ms, centered in the P-wave coda before the S-wave. RMS amplitude data show a strong correlation with pore pressure changes during the three pumping events.

Panel B shows the RMS amplitude computed using an evaluation window equal to Window P, from 13.2 ms to 14.9 ms, the P-wave first arrival, and used for computing the cross-correlation in the time delay analysis.